

Robust Generation Dispatch with Strategic Renewable Power Curtailment and Decision-Dependent Uncertainty

Yue Chen and Wei Wei

Abstract—As renewable energy sources replace traditional power sources (such as thermal generators), uncertainty grows while there are fewer controllable units. To reduce operational risks and avoid frequent real-time emergency controls, a preparatory schedule of renewable generation curtailment is required. This paper proposes a novel two-stage robust generation dispatch (RGD) model, where the preparatory curtailment schedule is optimized in the pre-dispatch stage. The curtailment schedule will then influence the variation range of real-time renewable power output, resulting in a decision-dependent uncertainty (DDU) set. In the re-dispatch stage, the controllable units adjust their outputs within the reserve capacities to maintain power balancing. To overcome the difficulty in solving the RGD with DDU, an adaptive column-and-constraint generation (AC&CG) algorithm is developed. We prove that the proposed algorithm can generate the optimal solution in finite iterations. Numerical examples show the advantages of the proposed model and algorithm, and validate their practicability and scalability.

Index Terms—generation dispatch, decision-dependent uncertainty, robust optimization, curtailment, adaptive C&CG

NOMENCLATURE

A. Abbreviations

C&CG	Column-and-constraint generation.
DDU	Decision-dependent uncertainty.
DRO	Distributionally robust optimization.
RG	Renewable generator.
RGD	Robust generation dispatch.
RO	Robust optimization.
SO	Stochastic optimization.

B. Indices, Sets, and Functions

\mathcal{AC}_n	Set of active constraints in iteration n .
$Q(p, r^\pm, w)$	The optimal objective value of the re-dispatch problem when the RG output is w .
$S(x, \xi)$	The optimal objective value of the inner “max-min” problem given the first-stage decisions x, ξ .
$S_f(x, \xi)$	The optimal objective value of the feasibility-check problem given the first-stage x, ξ .
$\mathcal{W}(\xi)$	Decision-dependent uncertainty set.

Y. Chen is with the Department of Mechanical and Automation Engineering, the Chinese University of Hong Kong, Hong Kong SAR (email: yuechen@mae.cuhk.edu.hk)

W. Wei is with the the State Key Laboratory of Power Systems, Department of Electrical Engineering, Tsinghua University, Beijing 100084 China. (wei-wei04@mails.tsinghua.edu.cn)

This work has been submitted to the IEEE for possible publication. Copyright may be transferred without notice, after which this version may no longer be accessible.

C. Parameters

d_i^\pm	Upward/Downward regulation cost coefficient of thermal unit i .
\mathcal{D}_{lt}	Demand of load l in period t .
F_k	Capacity of transmission line k .
N_g	Number of thermal units.
N_k	Number of transmission lines.
N_l	Number of loads.
N_w	Number of renewable generators.
P_i^u, P_i^l	Maximum/Minimum output of thermal unit i .
R_i^\pm	Maximum/Minimum reserve of thermal unit i .
$\mathcal{R}_i^d, \mathcal{R}_i^u$	Ramping limit of thermal unit i .
T	Number of dispatch periods.
u_{it}	Binary variable, $u_{it} = 1$ if the thermal unit i is on in period t ; otherwise $u_{it} = 0$.
W_{jt}^e	Forecast output of RG j in period t .
W_{jt}^u, W_{jt}^l	Upper/Lower bound of the confidence interval of power output of RG j in period t .
α_i	Running cost coefficient of thermal unit i .
β_i^\pm	Upward/Downward reserve cost coefficient of thermal unit i .
γ_j	Predispatch curtailment cost coefficient of RG j .
$\hat{\gamma}_j$	Redispatch curtailment cost coefficient of RG j .
$\pi_{ik}, \pi_{jk}, \pi_{lk}$	Line flow distribution factors.
Γ_S, Γ_T	Spatial/Temporal uncertainty budget.

D. Decision Variables

p_{it}	Contemporary output of thermal unit i in t .
p_{it}^\pm	Incremental outputs of thermal unit i in t .
r_{it}^\pm	Reserve capacity of thermal unit i in period t .
\hat{w}_{jt}	Output before pre-dispatch curtailment of RG j in period t .
w_{jt}	Output after pre-dispatch curtailment of RG j in period t .
w_{jt}^u, w_{jt}^l	The amount by which the power output of RG j deviates upward/downward from the forecast.
z_{jt}, \hat{z}_{jt}	Binary variables for linearization.
ξ_{jt}	Pre-dispatch curtailment of RG j in period t .
$\hat{\xi}_{jt}$	Redispatch curtailment of RG j in period t .

I. INTRODUCTION

ONE effective way to mitigate global warming is the massive deployment of renewable energy. In 2020, wind power with an incremental capacity of 93 GW was installed,

boosting the total global capacity to 743 GW [1]. Despite a decrease in energy consumption due to COVID-19 in 2020, the global cumulative solar capacity increased by 22%, establishing a new milestone for the solar sector [2]. At the same time, increasing renewable energy penetration poses a significant challenge to power system operations due to its intermittent, volatile, and uncertain characteristics. Generation dispatch (a generalization of economic dispatch) is widely used to deal with uncertainties by altering the real-time output of controllable generator within reserve capacity to hedge against renewable power output fluctuations [3].

The majority of existing research studies the generation dispatch problem under uncertainty using stochastic optimization (SO) [4], [5], robust optimization (RO) [3], [6], and distributionally robust optimization (DRO) [7], [8]. Stochastic optimization aims to minimize the expected cost or to meet certain chance constraints based on the assumption that the renewable generator (RG) output follows a known probability distribution. However, in practice, though we can obtain a rough histogram via historical data, it is hard to procure the exact probability distribution. Deviation from the real distribution may result in sub-optimal or even infeasible solutions. In contrast, RO considers all possible realizations of RG output in a prespecified uncertainty set and comes up with the dispatch strategy that minimizes the cost under the worst-case scenario. Various effective algorithms, such as Bender's decomposition [9] and column-and-constraint generation (C&CG) [10], were put forward to get the robust optimal solution efficiently. DRO is in-between SO and RO. Instead of using an uncertainty set, it describes the RG output by all possible probability distributions with the same mean and variance recovered from the historical data. Though DRO is less conservative than RO, it is time-consuming since it involves solving a semi-definite program [8]. Therefore, this paper adopts the robust generation dispatch (RGD) model.

In most existing literature, the uncertainty set in an RGD model is determined based on all available renewable generation, implicitly assuming that 100% of renewable generation can be used without curtailment. However, as renewable energy sources replace conventional power sources (e.g., thermal generators), uncertainty increases while there are fewer controllable units. As a result, curtailment of renewable energy is inevitable to maintain system security [11]. References [12] and [13] developed two-stage unit commitment models taking into account the wind power curtailment. However, the curtailment only happens in real-time without preparatory schedules. This paper focuses on future power systems with a high penetration of renewable energy. Real-time curtailment only could lead to the immediate shutdown of a large number of renewable generators, which may worsen system dynamic performance or trigger instability/oscillation [14]. Moreover, with more renewable generators and fewer thermal units, the power system inertia decreases, which will aggravate the risk of instability [15]. To deal with this challenge, in Spain, both the scheduled curtailment that is determined before the day-ahead market closes and the real-time curtailment have been applied [16]. Reference [14] also emphasized the need for considering curtailment in the pre-dispatch stage so that

we can have a relatively long time to make adjustments. Furthermore, the preparatory schedule of curtailment can help lower the amount of reserve required since the system is less unpredictable. For the reasons above, in this paper, we take into account preparatory curtailment in the pre-dispatch stage.

When the curtailment of renewable energy is incorporated in the pre-dispatch stage, the variation range of real-time RG output will be influenced. Therefore, distinct from the uncertainty sets in traditional robust optimization models that are pre-specified, the uncertainty set in our model depends on the first-stage decision. *Decision-dependent uncertainty* (DDU) has captured great attention in recent years and mainly two types of DDU have been considered [27]: 1) information structure related DDU (Type-1), i.e., decisions affect when knowledge about uncertain factors becomes available; 2) uncertainty distribution related DDU (Type-2), i.e., decisions affect the size of an uncertainty set or the chance that a scenario happens. Related studies are summarized in TABLE I. Stochastic programming was applied to deal with DDU [17]–[19]. As for robust optimization, reference [20] provided a reformulation method to solve the static robust model with DDU in which only “here-and-now” variables were included and the size of uncertainty set merely depends on binary variables. Another robust counterpart model was established in [21] with a more general set. In practice, adjustable robust optimization is more commonly used since it can describe the adjustment behaviors after the realization of uncertain factors. The solution of an adjustable robust optimization with DDU can be estimated via a K-adaptability approximation based algorithm [22]. Multi-parametric programming [23], modified Bender's decomposition [24], [25], and improved C&CG [26] were deployed to offer an exact solution. However, they are either time-consuming with a growing number of units or concentrated on the linear DDU set. In general, robust optimization with DDU is an important albeit challenging problem due to its computational intractability [28].

This paper proposes a robust generation dispatch model considering curtailment in the pre-dispatch stage. An adaptive C&CG algorithm is developed to solve the problem efficiently in finite iterations. Our main contributions are two-fold:

1) **Robust generation dispatch model with DDU.** A novel RGD model considering renewable power curtailment in the pre-dispatch stage is proposed. The pre-dispatch curtailment is defined as the upper limit of the actual RG output, which is co-optimized with the contemporary output and reserve capacity of thermal generators. This enables a preparatory schedule of curtailment and avoids frequent real-time emergency controls, which is more practical. Then in the re-dispatch stage, if the reserve is not enough to maintain power balancing, real-time curtailment will be executed. Distinct from the traditional RGD models, the variation range of RG output is capped by the pre-dispatch curtailment strategy, and so the uncertainty set is decision-dependent. Therefore, the proposed model renders a robust optimization with DDU. The nonlinear DDU set is further linearized into a mixed-integer linear set. Case studies show that the proposed model can avoid significant wind curtailment in the re-dispatch stage and can also lower the amount of reserve required.

TABLE I
 SUMMARY OF RECENT WORK ON DDU

Model	Reference	Types of DDU	Solution Methodology	
Stochastic optimization	[17]	Type-1	Non-anticipativity constraints	
	[18]	Type-1	Non-anticipativity constraints	
	[19]	Type-2	A quasi-exact solution approach	
Static robust	[20]	Type-2	Equivalent reformulation	
	[21]	Type-2	Equivalent reformulation	
Robust optimization	[22]	Type-1	K-adaptability approximation	
	[23]	Type-2	Multi-parametric programming	
	Adaptive robust	[24]	Type-2	Modified Bender's decomposition
		[25]	Type-2	Modified Bender's decomposition
		[26]	Type-2	Improved C&CG

2) **Adaptive C&CG Algorithm.** With decision-dependent uncertainty, the traditional robust optimization algorithms cannot be applied since the previously selected scenario may be outside of the uncertainty set as the pre-dispatch strategy changes. In this paper, an adaptive C&CG algorithm is developed. We add the active constraints under the worst-case scenario rather than the worst-case scenario itself to the master problem in each iteration. Two types of degeneracy that may occur during active constraints identification are addressed. When the pre-dispatch strategy changes, the scenario generated by the active constraints remains a vertex of the new uncertainty set. We prove that our algorithm can generate the robust optimal solution in finite iterations. Case studies show that our algorithm can greatly reduce the computational time compared with the nested C&CG (which may still be applied but without a theoretical guarantee of finite-step-ending).

The rest of this paper is organized as follows. Section II introduces the decision-dependent uncertainty set and the robust generation dispatch model. An adaptive C&CG algorithm is developed in Section III to solve the problem. Case studies are given in Section IV with conclusions in Section V.

II. MATHEMATICAL FORMULATION

We consider a two-stage generation dispatch problem for a system with N_g thermal generators, N_w renewable generators (RGs), and T dispatch periods. In the first-stage (*pre-dispatch stage*), the contemporary output and reserve capacity of thermal generators are determined based on the RG forecast outputs. Moreover, the preparatory curtailment of RGs is also considered to adapt to the increasing fluctuation due to higher renewable energy penetration. In the second-stage (*re-dispatch stage*), the operator adjusts the output of thermal generators within their reserve capacities and/or make additional real-time curtailments to maintain power balancing. In the following, we first introduce the RG output uncertainty set, which is influenced by the first-stage curtailment strategy. Then the robust generation dispatch model with DDU is proposed.

A. Decision-dependent uncertainty set

In this paper, preparatory curtailment of RGs is considered in the first-stage to avoid frequent calls for emergency controls

in real-time. The curtailment is defined as an upper limit of the actual RG output, denoted as $\xi_{jt}, \forall j, \forall t$. Denote the actual output and output after preparatory curtailment of RG j in period t as \hat{w}_{jt} and w_{jt} , respectively. Then, the uncertainty set $\mathcal{W}(\xi)$ is as follows, depending on the curtailment strategy ξ .

$$\mathcal{W}(\xi) = \left\{ w \left\{ \begin{array}{l} w_{jt} = \min\{\hat{w}_{jt}, \xi_{jt}\}, \forall j, \forall t \\ \hat{w}_{jt} = W_{jt}^e + w_{jt}^u - w_{jt}^l, \forall j, \forall t \\ 0 \leq w_{jt}^l, w_{jt}^u \leq W_{jt}^h, \forall j, \forall t \\ w_{jt}^l, w_{jt}^u = 0, \forall j, \forall t \\ \sum_{j=1}^{N_w} \frac{w_{jt}^l + w_{jt}^u}{W_{jt}^h} \leq \Gamma_S, \forall t \\ \sum_{t=1}^T \frac{w_{jt}^l + w_{jt}^u}{W_{jt}^h} \leq \Gamma_T, \forall j \end{array} \right. \right\} \quad (1)$$

where $W_{jt}^e = (W_{jt}^l + W_{jt}^u)/2$, $W_{jt}^h = (W_{jt}^u - W_{jt}^l)/2, \forall j, \forall t$.

The RG output after preparatory curtailment is the minimum of the actual RG output and the upper limit, as in the first constraint. The remaining constraints limit the deviation of the actual RG output that fluctuates within a range $[W_{jt}^l, W_{jt}^u]$, whose mean is the forecast value W_{jt}^e . When the RG output is higher than its forecast, $w_{jt}^u > 0, w_{jt}^l = 0$; otherwise, $w_{jt}^u = 0, w_{jt}^l > 0$. To avoid over-conservativeness of the model, uncertainty budgets Γ_S and Γ_T are added to restrain the spatial and temporal deviations from the prediction.

The above uncertainty set involves nonlinear constraints $w_{jt} = \min\{\hat{w}_{jt}, \xi_{jt}\}, \forall j, \forall t$, each of which can be linearized by introducing a binary variable as below.

$$w_{jt} \leq \hat{w}_{jt}, w_{jt} \leq \xi_{jt} \quad (2a)$$

$$\hat{w}_{jt} - (W_{jt}^u - W_{jt}^l)(1 - z_{jt}) \leq w_{jt} \quad (2b)$$

$$\xi_{jt} - (\xi_{jt} - W_{jt}^l)z_{jt} \leq w_{jt} \quad (2c)$$

$$z_{jt} \in \{0, 1\} \quad (2d)$$

when $z_{jt} = 0$, constraints (2a) and (2c) lead to $w_{jt} = \xi_{jt} \leq \hat{w}_{jt}$, while (2b) becomes $\hat{w}_{jt} - w_{jt} \leq W_{jt}^u - W_{jt}^l$ which is always satisfied. In this case, there is surplus RG output and curtailment is executed. When $z_{jt} = 1$, constraints (2a) and (2b) lead to $w_{jt} = \hat{w}_{jt} \leq \xi_{jt}$, while (2c) becomes $w_{jt} \geq W_{jt}^l$ which is always

satisfied. Thus, no RG output is curtailed. The other nonlinear constraint $w_{jt}^l w_{jt}^u = 0$ can be linearized as

$$0 \leq w_{jt}^l \leq M \hat{z}_{jt}, \quad 0 \leq w_{jt}^u \leq M(1 - \hat{z}_{jt}), \quad \hat{z}_{jt} \in \{0, 1\} \quad (3)$$

where M is a large constant.

After the above transformation, the uncertainty set (2) consists of mixed-integer linear constraints. Moreover, it relies on the value of the first-stage curtailment strategy ξ , and thus, is *decision-dependent*. Traditional algorithms for solving robust optimizations with decision-independent uncertainty set are the Bender's decomposition [9] and the C&CG algorithm [10]. However, they cannot be directly applied to solve the robust optimization with DDU due to the following two difficulties:

1) *Failure in robust feasibility and optimality*. When the first-stage decision changes, the previously selected scenarios may be outside of the new uncertainty set. For example, suppose w_1 is the worst-case scenario corresponding to a first-stage decision ξ_1 , i.e., $w_1 \in \mathcal{W}(\xi_1)$. Then when the decision changes to ξ_2 , we could have $w_1 \notin \mathcal{W}(\xi_2)$. Consequently, adding the scenario w_1 to the master problem may no longer result in a relaxation of the original robust optimization. This could lead to over-conservative or even infeasible solutions.

2) *Failure in finite convergence*. The proof of convergence of the C&CG algorithm is based on the fact that: the worst scenario always rests at a vertex of the uncertainty set, the same vertex will not be picked up twice, and the number of vertices is finite. However, when the uncertainty set becomes decision-dependent, the previously selected scenarios may no longer be at the vertex of the new set, and so there is no convergence guarantee.

In this paper, we develop an adaptive C&CG algorithm to address the above issues, which will be explained in detail in Section III.

B. Robust generation dispatch model

The robust generation dispatch model considering preparatory curtailment of RGs is given below:¹

$$\min_{p, r^{\pm}, \xi} \sum_{t=1}^T \sum_{i=1}^{N_g} (\alpha_i p_{it} + \beta_i^+ r_{it}^+ + \beta_i^- r_{it}^-) + \sum_{t=1}^T \sum_{j=1}^{N_w} \gamma_j (W_{jt}^u - \xi_{jt})^2 + \max_{w \in \mathcal{W}(\xi)} Q(p, r^{\pm}, w) \quad (4a)$$

$$\text{s.t. } W_{jt}^l \leq \xi_{jt} \leq W_{jt}^u, \quad \forall j \in [N_w], \quad \forall t \in [T] \quad (4b)$$

$$u_{it} P_i^l \leq p_{it} \leq u_{it} P_i^u, \quad \forall i \in [N_g], \quad \forall t \in [T] \quad (4c)$$

$$(p_{it} + r_{it}^+) - (p_{i(t-1)} - r_{i(t-1)}^-) \leq u_{i(t-1)} \mathcal{R}_i^u + (1 - u_{i(t-1)}) P_i^u, \quad \forall i \in [N_g], \quad \forall t \in [T] / \{1\} \quad (4d)$$

$$-(p_{it} + r_{it}^+) + (p_{i(t-1)} - r_{i(t-1)}^-) \leq u_{it} \mathcal{R}_i^d + (1 - u_{it}) P_i^u, \quad \forall i \in [N_g], \quad \forall t \in [T] / \{1\} \quad (4e)$$

$$(p_{it} - r_{it}^-) - (p_{i(t-1)} + r_{i(t-1)}^+) \leq u_{i(t-1)} \mathcal{R}_i^u + (1 - u_{i(t-1)}) P_i^u, \quad \forall i \in [N_g], \quad \forall t \in [T] / \{1\} \quad (4f)$$

$$-(p_{it} - r_{it}^-) + (p_{i(t-1)} + r_{i(t-1)}^+) \leq u_{it} \mathcal{R}_i^d$$

¹[A] denotes all positive integers that do not exceed A.

$$+ (1 - u_{it}) P_i^u, \quad \forall i \in [N_g], \quad \forall t \in [T] / \{1\} \quad (4g)$$

$$u_{it} P_i^l \leq p_{it} - r_{it}^-, \quad p_{it} + r_{it}^+ \leq u_{it} P_i^u, \quad \forall i \in [N_g], \quad \forall t \in [T] \quad (4h)$$

$$0 \leq r_{it}^- \leq u_{it} R_i^-, \quad 0 \leq r_{it}^+ \leq u_{it} R_i^+, \quad \forall i \in [N_g], \quad \forall t \in [T] \quad (4i)$$

$$\sum_{j=1}^{N_w} W_{jt}^e + \sum_{i=1}^{N_g} p_{it} = \sum_{l=1}^{N_l} \mathcal{D}_{lt}, \quad \forall t \in [T] \quad (4j)$$

$$-F_k \leq \sum_{i=1}^{N_g} \pi_{ik} p_{it} + \sum_{j=1}^{N_w} \pi_{jk} W_{jt}^e$$

$$- \sum_{l=1}^{N_l} \pi_{lk} \mathcal{D}_{lt} \leq F_k, \quad \forall k \in [N_k], \quad \forall t \in [T] \quad (4k)$$

The first-stage decisions, including the contemporary output $\{p_{it}, \forall i, \forall t\}$ and reserve capacity $\{r_{it}^{\pm}, \forall i, \forall t\}$ of thermal units, and the preparatory curtailment schedule $\{\xi_{jt}, \forall j, \forall t\}$, are made prior to the realization of uncertainty. The $\{u_{it}, \forall i, \forall t\}$ are binary parameters and $u_{it} = 1/0$ indicates the generator is on/off. Here, the unit commitment $\{u_{it}, \forall i, \forall t\}$ are given and fixed parameters. The objective function (4a) minimizes the sum of generation cost, reserve cost, preparatory curtailment cost, and the re-dispatch generation and curtailment costs under the worst-case scenario. The γ_j is a coefficient that fully incorporates the opportunity cost of renewable power curtailment, including but not limited to the resulting increased carbon emission, the impact on power system stability, and the possibility of exceeding the rate of renewable power spilling limits. A quadratic function that is widely used in literature, such as [29], is adopted. Denote the objective of the first-stage problem as f_s , then given the $\gamma_j > 0, \forall j$, we have

$$\frac{\partial f_s}{\partial \xi_{jt}} = -\gamma_j (W_{jt}^u - \xi_{jt}) \leq 0 < \frac{\partial f_s}{\partial p_{it}} = \alpha_i$$

According to equal incremental principle, it assures that renewable generators have higher priority compared with the thermal generators.

The curtailment strategy is between the lower and upper bounds of the actual RG output as in constraint (4b). Constraints (4c) and (4i) represent the limits of generation capacity and reserve capacity, respectively. Constraints (4d)-(4g) ensure that the ramping constraints still hold when offering the reserve capacities in the second-stage, so we do not need to consider the ramping rates in the second stage. The generation adequacy is ensured in (4h). Power balancing condition and power flow limits are given in (4j) and (4k), respectively. The term $Q(p, r^{\pm}, w)$ in (4a) is the re-dispatch cost when the RG output is w . Therefore, maximizing $Q(p, r^{\pm}, w)$ over all possible $w \in \mathcal{W}(\xi)$ gives the cost under the worst-case scenario. Here, $\mathcal{W}(\xi)$ is the decision-dependent uncertainty set (1). To be specific, $Q(p, r^{\pm}, w)$ is the optimal objective value of the second-stage re-dispatch problem:

$$\min_{p^{\pm}, \xi} \sum_{t=1}^T \sum_{i=1}^{N_g} (d_i^+ p_{it}^+ + d_i^- p_{it}^-) + \sum_{t=1}^T \sum_{j=1}^{N_w} \hat{\gamma}_j \hat{\xi}_{jt}^2 \quad (5a)$$

$$\text{s.t. } 0 \leq p_{it}^+ \leq r_{it}^+, \quad 0 \leq p_{it}^- \leq r_{it}^-, \quad \forall i \in [N_g], \quad \forall t \in [T] \quad (5b)$$

$$\hat{\xi}_{jt} \geq 0, \quad \forall i \in [N_w], \quad \forall t \in [T] \quad (5c)$$

$$\sum_{i=1}^{N_g} (p_{it} + p_{it}^+ - p_{it}^-) + \sum_{j=1}^{N_w} (w_{jt} - \hat{\xi}_{jt}) = \sum_{l=1}^{N_l} \mathcal{D}_{lt}, \quad \forall t \in [T] \quad (5d)$$

$$\begin{aligned}
 -F_k &\leq \sum_{i=1}^{N_g} \pi_{ik} (p_{it} + p_{it}^+ - p_{it}^-) + \sum_{j=1}^{N_w} \pi_{jk} (w_{jt} - \hat{\xi}_{jt}) \\
 -\sum_{l=1}^{N_j} \pi_{lk} \mathcal{D}_{lt} &\leq F_k, \quad \forall k \in [N_k], \quad \forall t \in [T]
 \end{aligned} \quad (5e)$$

The second-stage decisions, including the incremental outputs of thermal units $\{p_{it}^\pm, \forall i, \forall t\}$ and real-time curtailment $\{\hat{\xi}_{jt}, \forall j, \forall t\}$, are made after knowing the exact outputs of RGs. The objective function (5a) is to minimize the re-dispatch cost, i.e., the sum of up- and down-regulation costs and real-time curtailment costs. Constraint (5b) requires the incremental output of thermal unit be within its reserve capacity. Power balancing condition and power flow limits are (5d) and (5e). There is a quadratic term $\hat{\gamma}_j \hat{\xi}_{jt}^2$ in the objective function, which can be linearized via a convex combination approach [30]. To be specific, suppose we have evaluations at N discrete points $\xi_{jt}^1, \dots, \xi_{jt}^N$, and $\hat{g}_{jt}^1 = \hat{\gamma}_j (\xi_{jt}^1)^2, \dots, \hat{g}_{jt}^N = \hat{\gamma}_j (\xi_{jt}^N)^2$. By introducing variables $\sigma_{jt}^1, \dots, \sigma_{jt}^N \geq 0$ and $\sum_{n=1}^N \sigma_{jt}^n = 1$, $\hat{\xi}_{jt}$ and $\hat{\gamma}_j \hat{\xi}_{jt}^2$ can be replaced with linear functions $\sum_{n=1}^N \sigma_{jt}^n \xi_{jt}^n$ and $\sum_{n=1}^N \sigma_{jt}^n \hat{g}_{jt}^n$ in σ , respectively.

C. Compact form

The aforementioned robust generation dispatch model with decision-dependent uncertainty can be written in the following compact form:

$$\min_{x \in \mathbb{X}, \xi \in \Xi} c^\top x + g(\xi) + \max_{w \in \mathcal{W}(\xi)} \min_{y \in \mathbb{F}(x, w)} d^\top y \quad (6)$$

and

$$\begin{aligned}
 \mathbb{X} &= \{x \in \mathbb{R}^{3N_g \times T} : Ax \geq b\} \\
 \Xi &= \{\xi \in \mathbb{R}^{N_w \times T} : B\xi \leq e\} \\
 \mathcal{W}(\xi) &= \{w \in \mathbb{R}^{N_w \times T} : Hw \leq C\hat{w} + F\xi + Gz + a, \\
 &\quad \forall z \in \mathbb{Z}^{2N_w \times T}, \hat{w} \in \mathbb{R}^{3N_w \times T}\} \\
 \mathbb{F}(x, w) &= \{y \in \mathbb{R}^{(2N_g + N \times N_w) \times T} : Ey \leq f - Rw - Dx\} \quad (7)
 \end{aligned}$$

where $x := \{p_{it}, r_{it}^+, r_{it}^-, \forall i, \forall t\}$ and c is a collection of $\alpha_i, \beta_i^+, \beta_i^-, \forall i$. ξ is a collection of $\xi_{jt}, \forall j, \forall t$; $g(\xi) = (W^u - \xi)^\top \mathbf{diag}(\gamma_1, \dots, \gamma_{N_w})(W^u - \xi)$. $w := \{w_{jt}, \forall j, \forall t\}$, $\hat{w} := \{\hat{w}_{jt}, w_{jt}^l, w_{jt}^u, \forall j, \forall t\}$, and z is a collection of the binary variables z_{jt} and \hat{z}_{jt} for all j, t . $y := \{p_{it}^+, p_{it}^-, \forall i, \forall t; \sigma_{jt}^n, \forall j, \forall n, \forall t\}$; d summarizes $d_i^+, d_i^-, \forall i$ and $g_{jt}^n, \forall j, \forall n, \forall t$. $A, B, H, C, F, G, E, R, D$ and d, b, e, a, f are the coefficient matrices and vectors.

Remark: It is worth noting that the proposed model (6) subsumes the two-stage robust optimization with decision-independent uncertainty (DIU) as a special case. When F in $\mathcal{W}(\xi)$ is an all-zero matrix, the DDU set degenerates to a DIU set. The algorithm proposed in this paper can still be applied.

III. SOLUTION ALGORITHM

Different from the traditional robust optimization models [3], the uncertainty set in (6) is *decision-dependent*. The widely-used algorithms for solving the traditional robust optimizations may cause oscillation because the update of the first-stage decision keeps changing the shape as well as the extreme

points of the uncertainty set. In this section, an adaptive C&CG algorithm is proposed to generate the optimal solution in a finite number of iterations.

In this paper, we do not require relatively complete recourse, which assumes that the second-stage problem (5) is feasible for any fixed first-stage action x and scenario w . Instead, we assume that

A1: The robust optimization problem (6) has at least one *robust feasible* solution, i.e., there exists a $x \in \mathbb{X}, \xi \in \Xi$ such that for any $w \in \mathcal{W}(\xi)$, the second-stage problem (5) is always feasible.

This condition better matches engineering practices.

A. Equivalent transformation

Given the first-stage decisions $x \in \mathbb{X}$ and $\xi \in \Xi$, the inner “max-min” problem is a bilevel optimization:

$$S(x, \xi) := \max_{w \in \mathcal{W}(\xi)} \min_{y \in \mathbb{F}(x, w)} d^\top y \quad (8)$$

where $\mathbb{F}(x, w)$ is a polyhedral set while $\mathcal{W}(\xi)$ is bounded and consists of mixed-integer linear constraints depending on the value of ξ in the first-stage.

Note that the first-stage decisions $x \in \mathbb{X}$ and $\xi \in \Xi$ may not always be robust feasible. Therefore, we construct the following problem for feasibility-check first.

$$\begin{aligned}
 \min_s \quad & 1^\top s \\
 \text{s.t.} \quad & Ey \leq f - Rw - Dx + s, \quad s \geq 0
 \end{aligned} \quad (9)$$

where s is the slack variable. Obviously, the problem (9) is always feasible. If the original second-stage problem (5) is feasible, we have s is an all-zero vector with a zero optimal objective value; otherwise, the optimal objective value is larger than zero. Then the inner “max-min” problem for feasibility-check is equivalent to

$$\begin{aligned}
 S_f(x, \xi) &:= \max_{\substack{w \in \mathcal{W}(\xi), y, s, \\ \mu, \mu_s, z_\mu, z_{\mu_s}}} 1^\top s \\
 \text{s.t.} \quad & E^\top \mu = 0, \quad 1 - \mu - \mu_s = 0 \\
 & 0 \leq \mu \leq \hat{M} z_\mu, \quad 0 \leq \mu_s \leq \hat{M} z_{\mu_s} \\
 & 0 \leq (-Ey + f - Rw - Dx + s) \leq \hat{M}(1 - z_\mu) \\
 & 0 \leq s \leq \hat{M}(1 - z_{\mu_s}) \\
 & z_\mu, z_{\mu_s} \in \{0, 1\}^{n_\mu}
 \end{aligned} \quad (10)$$

where n_μ is the number of constraints in $\mathbb{F}(x, w)$, μ, μ_s are dual variables, and \hat{M} is a large enough constant. Problem (10) is obtained by replacing the problem (9) with its KKT condition and linearize the complementary and slackness condition in the form of $0 \leq x \perp y \geq 0$ using the Big-M method [31]. Then $S_f(x, \xi) = 0$ if and only if (x, ξ) is robust feasible. Denote the above optimization problem (10) as the feasibility-check problem **FCP**.

If (x, ξ) is robust feasible, we can then solve the original “max-min” problem (8), which is equivalent to

$$\max_{w \in \mathcal{W}(\xi), y, \mu, z_\mu} d^\top y \quad (11a)$$

$$\text{s.t.} \quad d + E^\top \mu = 0 \quad (11b)$$

$$0 \leq \mu \leq \hat{M}z_\mu \quad (11c)$$

$$0 \leq (-Ey + f - Rw - Dx) \leq \hat{M}(1 - z_\mu) \quad (11d)$$

$$z_\mu \in \{0, 1\}^{n_\mu} \quad (11e)$$

We denote the above optimization (11) as the subproblem **SP**.

Remark on the selection of the Big-M: The big-M method is applied for linearizing the constraint $w_{jt}^l w_{jt}^u = 0$ and also the complementary slackness condition in KKT. For the $w_{jt}^l w_{jt}^u = 0$, since both w_{jt}^l and w_{jt}^u are in $[W_{jt}^l, W_{jt}^u]$, we can just let $M = W_{jt}^u$. The complementary slackness condition in KKT is linearized using (11c)-(11e). The constraint $-Ey + f - Rw - Dx \geq 0$ refers to the physical constraints in problem (5), whose upper bounds can be derived according to their physical meanings. For example, for the constraint $p_{it}^+ - r_{it}^+ \leq 0$, we have $0 \leq r_{it}^+ - p_{it}^+ \leq r_{it}^+ \leq R_{it}^+$. The variable μ is the dual variable of the physical constraints, it reflects the marginal effect on the primal objective (5a) per unit change in the primal constraint limit. Therefore, the upper bound of μ can be obtained according to some sensitivity analysis on the power system beforehand. The big-M can be chosen as the maximum of the upper bounds for $-Ey + f - Rw - Dx$ and for μ . It's worth noting that a larger M is not always the better, since it may cause numerical instabilities. In the case study, we let $M = W_{jt}^u$ with $\hat{M} = 10^5$ for the IEEE 39-bus system and $\hat{M} = 10^6$ for the IEEE 118-bus system. All simulations can output the correct solutions efficiently.

Proposition 1. The optimal solution w^* of the problem **FCP** or **SP** will be reached at one of the extreme points of $\mathcal{W}(\xi)$.

Proof. Given x and ξ , the uncertainty set $\mathcal{W}(\xi)$ can be seen as the union of $2^{2N_w \times T}$ polytopes, each of which corresponds to a particular assignment to the set of binary variables $z \in \mathbb{Z}^{2N_w \times T}$, i.e., $\mathcal{W}(\xi) = \mathcal{W}^1(\xi) \cup \mathcal{W}^2(\xi) \cup \dots \cup \mathcal{W}^{2^{2N_w \times T}}(\xi)$. For the subproblem **SP**, $Q(x, w) := \min_{y \in \mathbb{F}(x, w)} d^\top y$ is a quasiconvex function in w , so the optimal solution of $\max_{w \in \mathcal{W}^p(\xi)} Q(x, w)$ will be achieved at the extreme point of $\mathcal{W}^p(\xi)$ [32]. The $\text{argmin}_{w \in \mathcal{W}^p(\xi)} Q(x, w), \forall p \in [2^{2N_w \times T}]$ with the highest objective value is the optimal solution of (8), which is also an extreme point of $\mathcal{W}(\xi)$. Similarly, we can prove the conclusion for the feasibility-check problem **FCP**. \square

Suppose the worst-case scenario identified by the **FCP** or the **SP** is w^* and the corresponding value of the binary variable is z^* . At the optimal point, the set of active and inactive constraints in $\mathcal{W}(\xi)$ are

$$H_{eq}w = C_{eq}\hat{w} + F_{eq}\xi + G_{eq}z + a_{eq} \quad (12)$$

$$H_{in}w < C_{in}\hat{w} + F_{in}\xi + G_{in}z + a_{in} \quad (13)$$

If we fix the value of z to z^* , then in non-degenerate cases, the matrix $[H_{eq}, -C_{eq}]$ is a $(4N_w \times T)$ -dimensional full rank matrix as the active constraints form a set of basis. For any given ξ , the value of (w, \hat{w}) can be uniquely determined by

$$\begin{bmatrix} w \\ \hat{w} \end{bmatrix} = [H_{eq}, -C_{eq}]^{-1} (F_{eq}\xi + G_{eq}z^* + a_{eq}) \quad (14)$$

However, in degenerate cases, it could be hard to recover w and \hat{w} using the active constraints. Methods to deal with this

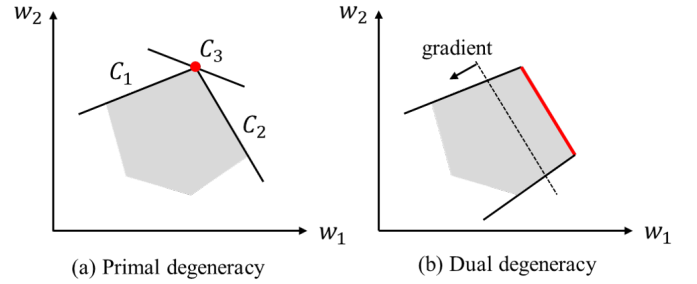


Fig. 1. Illustration of degenerate cases.

challenge are introduced in the following. Denote the set of active constraints we finally obtain in iteration n as \mathcal{AC}_n .

B. Model degeneracy

In general, two types of degeneracy may occur, i.e., primal degeneracy and dual degeneracy, which are illustrated in Fig. 1. Primal degeneracy is caused by weak redundant constraints. For example, in Fig. 1(a), constraints C1-C3 are all active at the optimal point so equation (12) is over-determined. In fact, constraint C3 is redundant: although C3 intersects the feasible region, removing C3 will not change the feasible region. The impact of primal degeneracy is manageable, because redundant constraints in $\mathcal{W}(\xi)$ can be filtered before identifying the active constraints, and then $[H_{eq}, -C_{eq}]$ is invertible. The method for removing redundant constraints is given in Appendix A. In particular, we need to be careful about three cases:

- 1) If $w_{jt}^* = W_{jt}^u$: In this case, we must have $w_{jt}^* = \xi_{jt}$; otherwise, we have $w_{jt}^* = \hat{w}_{jt}^* \leq \xi_{jt} \leq W_{jt}^u$. Equality holds for all inequalities in the middle, so we still have $w_{jt}^* = \xi_{jt} = W_{jt}^u$. Therefore, we have three active constraints $w_{jt} = \hat{w}_{jt}$ and $\hat{w}_{jt} = W_{jt}^e + w_{jt}^u - w_{jt}^l$, and $w_{jt}^l = 0$. Moreover, the active constraints $w_{jt}^u = W_{jt}^h$, and $w_{jt} = \xi_{jt}$ give the same limits and one of them is redundant. Our goal is to add the active constraint (12) to the master problem to ensure that when the first-stage decision changes, the scenario generated remains at the extreme point of the new set. To this end, here we remove the $w_{jt}^u = W_{jt}^h$.
- 2) If $\xi_{jt} = W_{jt}^l$ and $w_{jt}^* = W_{jt}^h$: Since $\hat{w}_{jt} = W_{jt}^e + w_{jt}^u - w_{jt}^l$ and $w_{jt}^u w_{jt}^l = 0$, we have $\hat{w}_{jt}^* = W_{jt}^l = \xi_{jt}$. Therefore, we have three active constraints $w_{jt} = \hat{w}_{jt}$, $\hat{w}_{jt} = W_{jt}^e + w_{jt}^u - w_{jt}^l$, and $w_{jt}^u = 0$. Moreover, the active constraints $w_{jt}^l = W_{jt}^h$ and $w_{jt} = \xi_{jt}$ give the same limits. For the reasons in 1), we remove the $w_{jt}^l = W_{jt}^h$.
- 3) If $\xi_{jt} = w_{jt}^e$ with $w_{jt}^{l*} = w_{jt}^{u*} = 0$: Since $\hat{w}_{jt} = W_{jt}^e + w_{jt}^u - w_{jt}^l$, we have $\hat{w}_{jt}^* = W_{jt}^e$. The two active constraints $w_{jt}^l = 0$ and $w_{jt}^u = 0$ gave the same limit as $w_{jt} = \xi_{jt}$. For the reasons in 1), we keep the $w_{jt} = \xi_{jt}$. For the constraint $w_{jt}^l = w_{jt}^u = 0$, due to the complementary condition $w_{jt}^l w_{jt}^u = 0$, we keep one of them and remove the other.

Dual degeneracy occurs if multiple solutions attain the optimal value, then the optimal solution is not unique. As in Fig. 1(b), a facet is perpendicular to the gradient of the

objective function, so any point on the facet is an optimal solution. When there is dual degeneracy, the matrix $[H_{eq}, -C_{eq}]$ is not full-rank, and (12) is underdetermined. We can include some of the constraints in (13) to make $[H_{eq}, -C_{eq}]$ a full rank matrix, i.e., letting $H_{in,j}w = C_{in,j}\hat{w} + F_{in,j}\xi + G_{in,j}z^* + a_{in,j}$ for some j . If the unique w^* and \hat{w}^* we get satisfy constraint (13), then use the new set of constraints as the active constraint.

C. Master Problem

The master problem (MP) in iteration N is formulated as

$$\min_{x, \xi} c^\top x + g(\xi) + \eta \quad (15a)$$

$$\text{s.t. } x \in \mathbb{X}, \xi \in \Xi \quad (15b)$$

$$\eta \geq d^\top y^n, \forall n \in [N] \quad (15c)$$

$$H_{eq}^n \tilde{w}^n = C_{eq}^n \hat{w}^n + F_{eq}^n \xi + G_{eq}^n z^{n*} + a_{eq}^n, \forall n \in [N] \quad (15d)$$

$$w^n = \min\{\tilde{w}^n, \xi\}, w^n = \max\{W^l, \tilde{w}^n\}, \forall n \in [N] \quad (15e)$$

$$y^n \in \mathbb{F}(x, w^n), \forall n \in [N] \quad (15f)$$

The decision variables are $\{x, \xi, \eta, y^n, w^n, \hat{w}^n, \tilde{w}^n, \forall n \in [N]\}$. n is the index of scenarios. w^n is the RG output scenario in the n -th iteration while \tilde{w}^n and \hat{w}^n are intermediate variables. The constraints of the first-stage problem are given in (15b). Since η is minimized in the objective (15a), constraint (15c) is equivalent to $\eta = \max_n \min_n d^\top y^n$ which is the re-dispatch cost under the worst-case scenario. The constraints in the second-stage problem are given in (15f). Our key innovation lies in the scenario representation (15d)-(15e). Instead of adding the worst-case scenario in the previous iteration itself directly to the master problem as the traditional robust optimization methods [10], here we include the set of active constraints (15d). When the first-stage decision ξ changes, the \tilde{w}^n will change accordingly and can be uniquely determined by (15d). Together with (15e), we can ensure that the scenario w^n is still an extreme point of $\mathcal{W}(\xi)$. We will give an example to explain this in detail in the Remark later.

The constraint $w^n = \min\{\tilde{w}^n, \xi\}$ can be linearized as

$$W^l \leq \tilde{w}^n \leq W^u, z_w^n \in \{0, 1\}^{N_w \times T} \quad (16a)$$

$$w^n \leq \tilde{w}^n, w^n \leq \xi \quad (16b)$$

$$\tilde{w}^n - (W^u - W^l)z_w^n \leq w^n \quad (16c)$$

$$\xi - (W^u - W^l)(1 - z_w^n) \leq w^n \quad (16d)$$

When $\tilde{w}^n \leq \xi$, let $z_w^n = 0$, constraint (16c) turns into $\tilde{w}^n \leq w^n$. Together with (16b), we have $w^n = \tilde{w}^n = \min\{\tilde{w}^n, \xi\}$. Moreover, constraint (16d) becomes $\xi - (W^u - W^l) \leq w^n$, which is satisfied since both ξ and \tilde{w}^n are in $[W^l, W^u]$. When $\tilde{w}^n \geq \xi$, let $z_w^n = 1$, constraint (16d) turns into $\xi \leq w^n$. Together with (16b), we have $w^n = \xi = \min\{\tilde{w}^n, \xi\}$. Moreover, constraint (16c) becomes $\tilde{w}^n - (W^u - W^l) \leq \xi$, which is satisfied since both ξ and \tilde{w}^n are in $[W^l, W^u]$.

This is different from the linearization technique in (2) since now ξ is a variable instead of a constant. Constraint $w^n = \max\{W^l, \tilde{w}^n\}$ can be linearized in a similar way since it is equivalent to $-w^n = \min\{-W^l, -\tilde{w}^n\}$. The master problem MP is thus turned into a mixed-integer quadratic program (MIQP) that can be solved efficiently by commercial software.

Remark: Since $[H_{eq}^n, -C_{eq}^n]$ is a full-rank matrix, \tilde{w}^n and \hat{w}^n can be uniquely represented as a function of ξ . If \tilde{w}^n is a feasible point of the new $\mathcal{W}(\xi)$, then we have $\tilde{w}^n \leq \xi$ and $\tilde{w}^n \geq W^l$ due to the constraints in $\mathcal{W}(\xi)$. Therefore, $w^n = \tilde{w}^n$ is an extreme point of the new $\mathcal{W}(\xi)$. If \tilde{w}^n is infeasible for the new $\mathcal{W}(\xi)$, then constraint (15e) projects it onto an extreme point (vertex) of the new $\mathcal{W}(\xi)$. We use a simple example with two RGs for illustration:

Suppose $T = 1$ and the uncertainty set is ²

$$\mathcal{W}(\xi) = \left\{ (w_1, w_2)^\top \left| \begin{array}{l} w_j = \min\{\hat{w}_j, \xi_j\}, \forall j = 1, 2 \\ \hat{w}_j = 4 + w_j^u - w_j^l, \forall j = 1, 2 \\ 0 \leq w_j^u, w_j^l \leq 2, \forall j = 1, 2 \\ \frac{w_1^l + w_1^u}{2} + \frac{w_2^l + w_2^u}{2} \leq \frac{3}{2} \end{array} \right. \right\} \quad (17)$$

Suppose in the $N - 1$ iteration, $\xi_1 = \xi_2 = 6$, so the feasible region is the grey region in Fig. 2(a). Suppose the optimal solution of the SP is point A. Primal degeneracy happens in this case and the constraints $w_2 \leq \xi_2$ and $w_2 \leq 6$ give the same limit. According to Section III-B, we keep the former constraint and drop the latter one. Therefore, the scenario A can be represented as a function of ξ , i.e. $(\tilde{w}_1, \tilde{w}_2) = (11 - \xi_2, \xi_2)$. Then in the N iteration, if $\xi = (6, 5.5)$ as in Fig. 2(b), the active constraints remain unchanged. Substituting the value of ξ into the expression of point A, we can get a new point A $(\tilde{w}_1, \tilde{w}_2) = (5.5, 5.5)$, which is a vertex of the new $\mathcal{W}(\xi)$. If $\xi = (5.5, 4.5)$ as in Fig. 2(c), now the new point A is $(\tilde{w}_1, \tilde{w}_2) = (6.5, 4.5)$ which is outside of $\mathcal{W}(\xi)$. But with constraint (15e), the point A (\tilde{w}) is projected to point A' (w) which is again a vertex of the new set $\mathcal{W}(\xi)$.

D. Adaptive C&CG algorithm

The overall iterative algorithm is given in Algorithm 1.

Theorem 1. The Algorithm 1 generates the optimal solution to problem (6) in finite iterations.

The proof of Theorem 1 can be found in Appendix B. The necessity and novelty of the proposed algorithm are highlighted below by comparing with two related algorithms.

- 1) **Nested C&CG** [33]. If we let \hat{w} be the variable of the middle ‘‘max’’ problem and move the constraint $w = \min\{\hat{w}, \xi\}$ to the inner ‘‘min’’ problem. The problem obtained is equivalent to the original robust optimization model (6) while the new uncertainty set becomes decision-independent. The nonlinear constraint $w = \min\{\hat{w}, \xi\}$ in the inner ‘‘min’’ can be linearized as

$$\begin{aligned} w &= \hat{w}z + \xi(1 - z) \\ w &\leq \hat{w}, w \leq \xi, z \in \{0, 1\}^{N_w \times T} \end{aligned} \quad (18)$$

Therefore, the problem is turned into a robust optimization problem with DIU and integer variables in the second stage. Denote the optimal value of the inner ‘‘min’’ as $Q(x, \hat{w})$. Nested C&CG [33] might be applied to solve this problem. However, since $Q(x, \hat{w})$ is not quasiconvex in \hat{w} , there is no guarantee that the optimal solution of the

²The t index is omitted for simplicity.

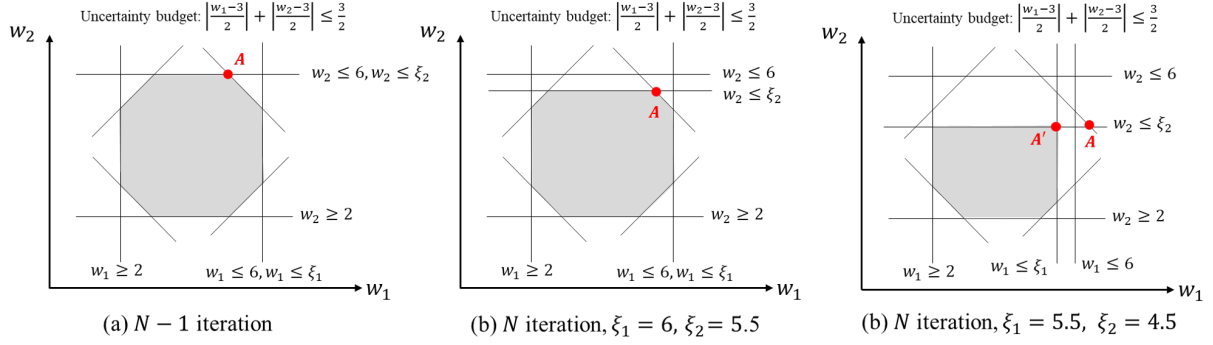


Fig. 2. Illustration of the adaptive RG power output scenario.

Algorithm 1: : Adaptive C&CG Algorithm

- 1: **Initiation:** Error tolerance $\varepsilon > 0$; $N = 1$; Let $C_{eq}^N, F_{eq}^N, G_{eq}^N$ be zero matrices; Let H_{eq}^N be an identity matrix and $a_{eq}^N = W^e$; Assign a large value to UB_0 .
 - 2: **Solve the Master Problem**
Solve the MP (15). Let (x^{N*}, ξ^{N*}) be the optimal solution and LB_N be the optimal value.
 - 3: **Feasibility-Check**
Solve the FCP (10) with (x^{N*}, ξ^{N*}) . If $S_f(x^{N*}, \xi^{N*}) = 0$, go the Step 4; otherwise, let \hat{w}^{N*} be the worst-case scenario and let $UB_N = UB_{N-1}$, go to Step 5.
 - 4: **Solve the Subproblem**
Solve the SP (11) with (x^{N*}, ξ^{N*}) . Let $(w^{N*}, \hat{w}^{N*}, z^{N*}, y^{N*})$ be the optimal solution and $UB_N = c^\top x^{N*} + g(\xi^{N*}) + d^\top y^{N*}$, go to Step 5.
 - 5: **Retrieve the active constraints**
Reduce redundant constraints (see Appendix A).
Deal with degenerate cases (see Section III-B).
Identify the set of active constraints \mathcal{AC}_N based on (12).
 - 6: if $|UB_N - LB_N| \leq \varepsilon$ and $S_f(x^{N*}, \xi^{N*}) = 0$, terminate and output (x^{N*}, ξ^{N*}) . Otherwise, $N = N + 1$, go to Step 2.
-

“max-min” will reside at one extreme point (vertex) of the DIU set. Therefore, the algorithm may not terminate in finite steps. In case studies, we use nested C&CG for comparison. The results show that, apart from the convergence issue, our method can greatly reduce the computational time compared with nested C&CG.

- 2) **Modified Bender’s decomposition** [24]. The method in [24] deals with the robust optimization problem with a linear decision-dependent uncertainty set. Instead of adding the worst-case scenario to the master problem in each iteration, the corresponding dual variables are added with constraints to ensure that w will be the optimal solution of the inner “max-min” problem with the selected dual variable. This constraint is equivalently represented as the KKT condition of the middle “max” problem so that the master problem renders a mixed integer linear program. However, for the model in this paper, the uncertainty set is a mixed-integer linear set, and we cannot get its KKT condition.

Remark: The proposed algorithm can also be applied to solve a robust optimization under DDU with integer variables in the inner level. The integer variables in the inner level will only affect the solution methodology for the “max-min” (8) (and the corresponding feasibility-check problem). Denote the integer variables by τ , whose feasible set is Υ . Then the “max-min” problem can be formulated as

$$\begin{aligned} \max_{w \in \mathcal{W}(\xi)} \quad & \min_{\tau, y} d^\top y \\ \text{s.t.} \quad & Fy \leq f - Rw - Dx - \tilde{E}\tau, \quad \tau \in \Upsilon \end{aligned} \quad (19)$$

Instead of replacing the inner minimization problem with its KKT condition, we can separate the integer variable from the continuous variable and turn the problem (19) to the following tri-level optimization problem.

$$\begin{aligned} \max_{w \in \mathcal{W}(\xi)} \quad & \min_{\tau \in \Upsilon} \min_y d^\top y \\ \text{s.t.} \quad & Fy \leq f - Rw - Dx - \tilde{E}\tau \end{aligned} \quad (20)$$

For the problem (20), take w as the first-stage decision variable, τ as the uncertain factor and Υ as the uncertainty set, and y as the second-stage decision variable, then the C&CG algorithm can be embedded to solve it.

IV. ILLUSTRATIVE EXPERIMENTS

We first use the IEEE-39 bus system with a single period for demonstration. Then the IEEE-118 bus system and the real Guangdong power grid of China are tested to show the scalability and practicability of the proposed method. Detailed data can be found in [34].

A. IEEE-39 bus system

The IEEE-39 bus system has 10 thermal generators and 46 transmission lines. The parameters of the thermal generators are given in TABLE II. There are three RGs connected to the power grid at nodes 4, 14, 29, respectively. Their forecast outputs are $W^e = [150, 150, 150]^\top$ MW and $W^l = 0.5W^e, W^u = 1.5W^e$. The uncertainty budget $\Gamma_S = 2$. The proposed Adaptive C&CG (AC&CG) algorithm and the Nested C&CG (NC&CG) algorithm are applied to solve the RGD problem, respectively. The change of UB_N and LB_N during iterations are given in Fig. 3. Note that the number of iterations of NC&CG in

TABLE II
PARAMETERS OF THE THERMAL GENERATORS

Unit	P_i^l (MW)	P_i^u (MW)	R_i^\pm (MW)	α_i (\$/MW)	β_i^\pm (\$/MW)	d_i^\pm (\$/MW)
1	70	155	120	16.19	1.62	1.62
2	70	155	120	17.26	1.73	1.73
3	40	80	60	16.60	1.66	1.66
4	30	50	50	16.50	1.59	1.59
5	55	100	70	19.70	1.97	1.97
6	30	50	30	22.26	2.22	2.22
7	25	55	34	22.74	2.77	2.77
8	20	55	22	25.92	2.59	2.59
9	20	55	20	27.27	2.73	2.73
10	20	55	10	27.79	1.30	1.30

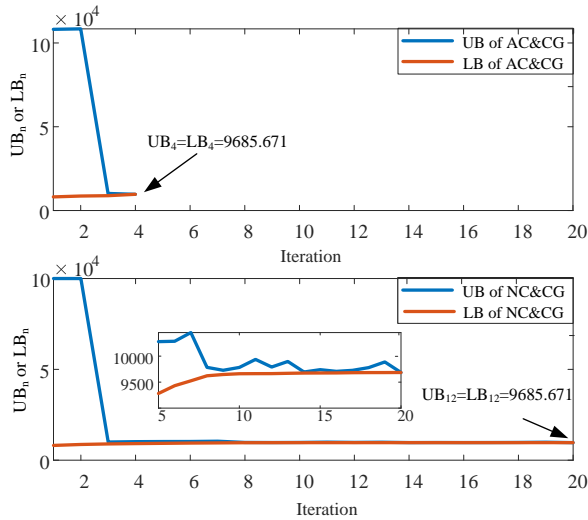


Fig. 3. Values of UB_N and LB_N during iterations.

Fig. 3 and TABLE VI refer to the number of outer-loops for adding the worst-case scenarios to the master problem. We can find that both algorithms output the same solution with an optimal objective value of \$9,685.671 and the curtailment strategy $\xi = [195.00, 200.00, 175.00]^T$ MW. This verifies the proposed algorithm. The NC&CG algorithm takes 41.79s to converge while the AC&CG takes 2.61s. The proposed AC&CG algorithm can greatly reduce the computational time since it only requires 4 iterations to reach the optimal solution whereas the NC&CG takes 20 iterations. Let alone the fact that in each iteration, the NC&CG algorithm takes another 3-4 iterations to solve the subproblem.

The decision-dependent uncertainty set in the 1st, 3rd, and 4th iterations are shown in Fig. 4. When the first-stage decision changes, the uncertainty set changes dramatically. As a result, a previously picked scenario, for example if it is point A, may fall outside of the uncertainty set. Continuing to use traditional robust optimization algorithms may result in over-conservative or infeasible results. This demonstrates the necessity of this work. The worst-case scenarios selected during the iterations of the two algorithms are plotted in Fig. 5 and Fig. 6, respectively. In each iteration, a different background color represents a different set of active constraints.

In Fig. 5, the same set of active constraint recurs. For

example, in the 7th - 20th iterations, the worst-case scenarios are generated by the same active constraint $w = \xi$. This is the root of the inefficiency of traditional algorithms: when the first-stage decision changes, the previously selected scenario may no longer be a vertex of the new uncertainty set. Therefore, there are an infinite number of possible uncertain scenarios and the algorithm does not necessarily stop in a finite number of steps. In contrast, in Fig. 6, the same set of active constraints appears only once. Instead of a fixed value, the previously selected scenario will change with the first-stage decision. The set of selected scenarios after the 2nd, 3rd, and 4th iterations are connected by the solid line, dashed line, and dash-dot line, respectively. For example, the scenario identified in the 2nd iteration is $w_2^* = [150, 225, 225]^T$ MW, and thus, the active constraints are $w_2^2 = \xi_2$, $w_3^2 = \xi_3$, and $w_1^2 = w_2^2 + w_3^2 - 300$. In the 3rd iteration, it changes to $w_2^3 = [131.34, 218.78, 212.56]^T$ since the curtailment strategy changes to $\xi = [225, 218.78, 212.56]^T$ MW. Then as the curtailment strategy changes to $\xi = [195.00, 200.00, 175.00]^T$ MW in the 4th iteration, the scenario further changes to $w_2^4 = [75.00, 200.00, 175.00]^T$ MW.

To show the advantages of the proposed model (Model-1), we compare it with the one that merely uses re-dispatch curtailment (Model-2). The Model-2 is derived by fixing ξ_{jt} in the proposed model to W_{jt}^u for all $j \in [N_w], t \in [T]$. Since ξ is now a constant, Model-2 is a robust optimization with decision-independent uncertainty. We test the performance of the two models under different maximum reserve limits. The results are shown in TABLE III. We can find that with the proposed model, the reserve cost can always be reduced. For example, in the case with R_i^\pm , the reserve cost is decreased by $(461.9 - 442.2)/461.9 = 4.3\%$. Moreover, the real-time curtailment in the proposed model is much smaller than that in Model-2, so the system dynamic characteristics do not change significantly, reducing the risk of instability. The total cost of the proposed model is substantially lower than that of Model-2, and with a more stringent reserve limit, the cost reduction becomes more significant.

Out-of-sample test is also conducted to evaluate the performance of the proposed model in terms of feasibility and cost. We randomly generate scenarios from a normal distribution with the mean of W_{jt}^e and the standard variance of 30, 40, 50, respectively. Five hundred scenarios are tested for each setting and the number of infeasible scenarios, the expected re-dispatch cost, and the worst-case real-time curtailment are recorded in TABLE IV. We can find that the proposed model can achieve a similar performance to the Model-2 in robustness but with a lower expected re-dispatch cost. Moreover, the worst-case real-time curtailment of the proposed model is much smaller than that of Model-2, meaning that the proposed model is posing less pressure on the real-time power system operation.

B. IEEE-118 bus system: Benchmark

We further test the performance of our proposed algorithm using a larger IEEE-118 bus system. There are 54 thermal generators and 186 transmission lines. Our proposed algorithm

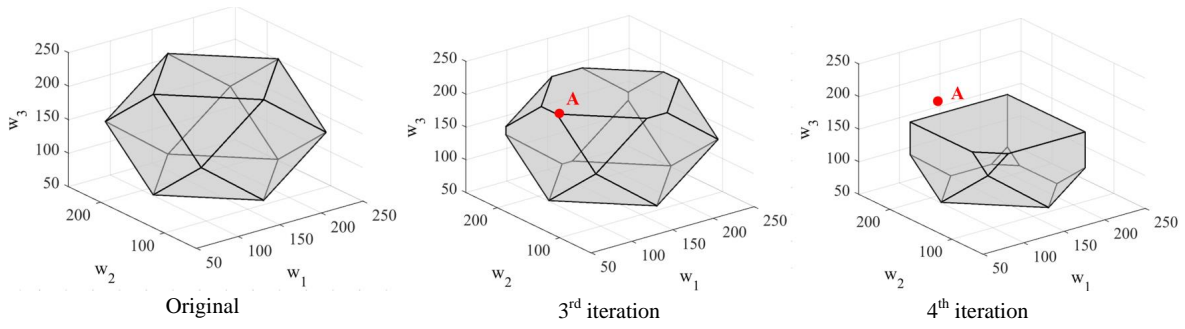


Fig. 4. Decision-dependent uncertainty sets.

TABLE III
COMPARISON OF THE PROPOSED MODEL AND MODEL-2

	R_i^\pm		$0.5R_i^\pm$		$0.3R_i^\pm$	
	Model-1	Model-2	Model-1	Model-2	Model-1	Model-2
Generation cost (\$)	8,129.3	8,129.3	8,143.0	8,149.6	8,215.7	8,215.7
Reserve cost (\$)	442.2	461.9	450.8	468.1	465.6	465.6
Pre-dispatch curtailment cost (\$)	787.5	0	787.5	0	787.5	0
Redispatch cost (\$)	183.9	177.9	179.3	180.0	187.5	187.5
Re-dispatch curtailment Amount (MW) / Cost (\$)	4.76/142.7	39.91/1,146.0	9.91/148.7	39.91/1,146.0	9.91/148.7	39.91/1,146.0
Total cost (\$)	9,685.6	9,915.1	9,709.3	9,943.7	9,805.0	10,014.8

TABLE IV
OUT-OF-SAMPLE TEST OF THE PROPOSED MODEL AND MODEL-2

	Standard variance		30		40		50	
	Model-1	Model-2	Model-1	Model-2	Model-1	Model-2	Model-1	Model-2
Infeasible scenarios	22/500	25/500	42/500	46/500	55/500	68/500		
Expected re-dispatch cost (\$)	106.74	107.12	111.10	116.28	120.17	127.46		
Worst-case real-time curtailment (MW)	9.91	173.59	9.91	308.30	9.91	371.61		

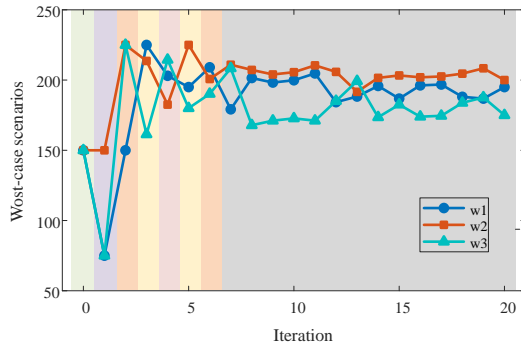


Fig. 5. Worst-case scenarios during iterations of the nested C&CG.

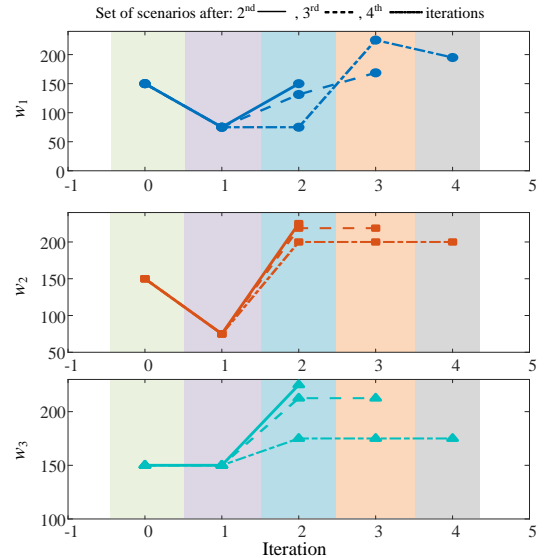


Fig. 6. Worst-case scenarios during iterations of our proposed algorithm.

(AC&CG) takes 6 iterations (35.17 seconds) to reach the robust optimal solution. The traditional nested C&CG takes 13 iterations (418.22 seconds). The change of UB_N and LB_N are given in Fig. 7. Since UB_N and LB_N vary in a wide range, therefore, we draw the $\log(UB_N)$ and $\log(LB_N)$ instead. Both algorithms output the same result while the proposed algorithm can greatly reduce the computational time.

The optimal curtailment strategy (ξ^*) as well as the upper/lower bound of the net load ($\sum_l D_{lt} - \sum_i p_{it}$) and the RG power output ($\sum_j w_{jt}$) is shown in Fig. 8. With growing

renewable energy penetration, in many periods (e.g., 1-19h), the upper bound of the total RG power output is much higher than the upper bound of the net load, i.e., $W^u > \sum_l D_{lt} - \sum_i P_{it}^l$. Therefore, preparatory curtailment is required to avoid poten-

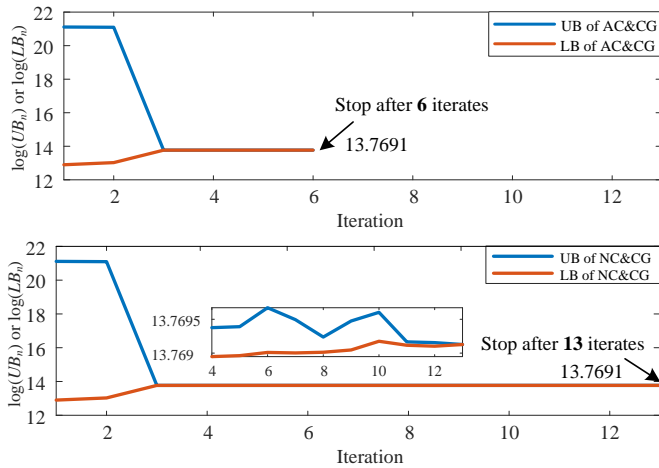
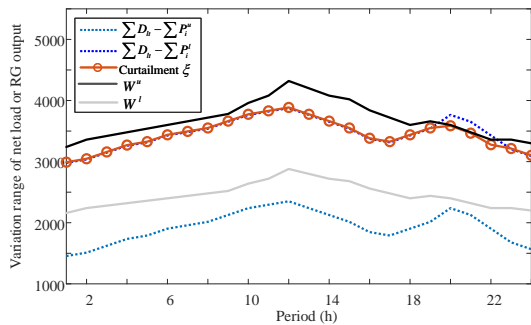

 Fig. 7. Values of $\log(UB_N)$ and $\log(LB_N)$ during iterations.


Fig. 8. Curtailment schedule and variation range of net load and RG output.

tial risks brought by a large amount of real-time curtailment; and correspondingly, the red curve in Fig. 8 is lower than the upper black curve (W^u). In hours 20 and 21, the maximum net load is higher than the maximum RG power output, and there is no need of preparatory curtailment. However, in hour 22, even though the maximum net load is higher than the maximum RG power output, pre-dispatch curtailment still occurs, which is caused by the ramping capacity limit. From Fig. 8 we can find that, curtailment happens in most of the time, and if all are done in real-time without a preparatory schedule, it will result in frequent emergency controls that will jeopardize the system's stability. That's why we need to decide on the curtailment schedule in the pre-dispatch stage.

Four typical scenarios are selected from the uncertainty set in the last iteration of the nested C&CG algorithm and the proposed algorithm, respectively. They are plotted in Fig. 9 together with the optimal pre-dispatch curtailment strategy ξ . When applying the nested C&CG algorithm, we move the $w = \min\{\hat{w}, \xi\}$ constraint to the inner "min" problem and turn the uncertainty set into a decision-independent one, which is the shaded area in Fig. 9(a) (for more details, please refer to Section III-D). First, we can find that scenarios 1, 2, and 4 exceed the upper limit imposed by the curtailment schedule. Thus, they are not feasible for the original decision-dependent uncertainty set (1) and this makes the traditional C&CG not applicable. Moreover, the selected scenarios (e.g. scenarios

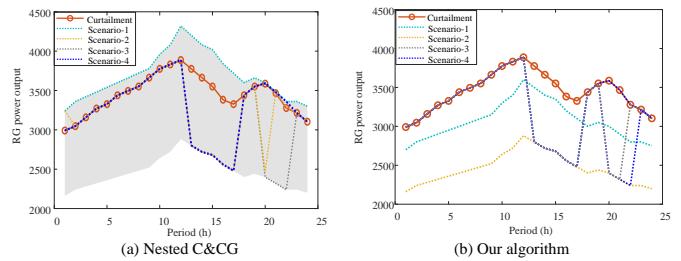


Fig. 9. Selected worst-case scenarios under two algorithms.

 TABLE V
 COSTS AND TIMES UNDER DIFFERENT RAMPING LIMITS

Ratio	First/Second stage curtailment	reserve cost	total cost	Time
1.0	5,610.4 / 160.0	32,668.5	954,675.6	35.17
1.3	5,543.3 / 170.0	31,195.9	936,187.3	46.74
1.5	5,533.3 / 214.0	30,483.7	930,556.1	39.60
2.0	5,533.9 / 210.0	28,626.8	924,994.1	18.57
2.5	5,533.9 / 210.0	27,961.5	924,266.8	22.04
3.0	5,533.9 / 210.0	27,961.5	924,266.8	29.47

2 and 3) may not be vertices of the decision-independent uncertainty set (shaded area). Therefore, there is no guarantee that the nested C&CG algorithm will stop after a finite number of iterations. In contrast, under the proposed algorithm, the previously selected algorithm can change adaptively and all remains feasible for the new uncertainty set as in Fig. 9(b).

C. IEEE-118 bus system: Impact of different factors

In the following, we analyze the impact of several factors. First, we change the ramping limit $\mathcal{R}_i^u, \mathcal{R}_i^d, \forall i$ from 1.0 to 3.0 times of their original values. The results are shown in TABLE V. With a tighter limit, the system operator has to use more costly generators for reserve, so the reserve cost increases. To cope with this, we want to reduce the uncertainty faced by the system, so that less reserve will be needed. The level of uncertainty can be reduced by planning most of the curtailment in advance. For example, the total curtailment in the case with ratio=1.0 is similar to that in the case with ratio=3.0. But in the former case, more curtailment are prepared beforehand. With more renewable generators replace the conventional generators, the ramping capacity will become more scarce, and thus, preparatory curtailment is more imperative. When the ratio changes from 2.0 to 2.5, even though the curtailments are the same, the total cost declines. This is because larger ramping limits enable a better allocation of contemporary output and reserve capacity of thermal units. When the ratio changes from 2.5 to 3.0, both the curtailment cost and total cost remain unchanged since ramping limits are no longer binding factors. Moreover, the computational times are all acceptable.

Furthermore, we test the performance of the two algorithms under different levels of uncertainty as given in TABLE VI. When the uncertainty decreases, both the curtailment amount and the total cost decline, which is straightforward. With

TABLE VI
CURTAILMENTS AND TIMES UNDER DIFFERENT UNCERTAINTY LEVELS

$[W^l, W^u]$	First/Second stage curtailment	AC&CG / NC&CG	
		No. of iterates	Time (s)
$[0.80, 1.20]W^e$	5,610.4 / 160.0	6 / 13	35.17 / 418.22
$[0.85, 1.15]W^e$	2,646.3 / 93.2	5 / 27	46.19 / 861.09
$[0.90, 1.10]W^e$	885.6 / 23.7	7 / 17	82.00 / 240.46
$[0.95, 1.05]W^e$	142.7 / 84.3	3 / 3	16.53 / 23.18
$[1.00, 1.00]W^e$	0.0 / 0.0	1 / 1	2.01 / 3.49

TABLE VII
TOTAL COST AND COMPUTATIONAL TIME OF THE GUANGDONG SYSTEM

Γ_T	16	18	20	22	24
Total cost (\$)	170,416,392	170,660,423	170,864,676	171,019,459	171,134,996
Iteration	6	6	5	5	3
Time (s)	1075.1	911.0	591.8	154.1	43.2

higher uncertainty, the number of iterations needed by the proposed AC&CG algorithm is stable while that taken by the NC&CG is less predictable. This shows the superiority of the proposed algorithm in the future power system with severe renewable energy fluctuations.

D. Guangdong Power System

The real Guangdong power grid of China is also tested to show the scalability of the proposed approach. The whole system has 1880 buses, 2452 transmission lines, 174 thermal generators, 453 loads, and six in planning large-scale wind farms located at Guangzhou, Shaoguan, Shenzhen, Dongguan, Shantou, and Zhanjiang, respectively. The predicted nodal loads in a normal winter day are used in this test. We change the uncertainty budget Γ_T from 18 to 24 and record the total cost, number of iterations, and computational times in TABLE VII. We can find that the computational times are less than 18min, which is acceptable. The optimal pre-dispatch curtailment and the worst-case scenarios of the case with $\Gamma_T = 20$ are shown in Fig. 10. With the pre-dispatch curtailment ξ , the variation range of renewable power output (capped by ξ) is smaller than the original region $[W^l, W^u]$ (the grey area). All selected scenarios remain within the decision-dependent uncertainty set $\mathcal{W}(\xi)$, which validates the theoretical analysis.

V. CONCLUSION

In this paper, a novel RGD model considering preparatory schedule of renewable power curtailment is proposed. The model casts down to a robust optimization with DDU. An adaptive C&CG algorithm was developed to solve the problem efficiently by identifying the active constraints in each iteration and adding them to the master problem. In this way, the worst-case scenarios remain to be vertices of the uncertainty set when the first-stage decision changes. Our main findings are:

1) We prove theoretically that the proposed algorithm can generate the robust optimal solution in a finite number of iterations. Many of the existing algorithms do not have this guarantee due to the decision-dependent uncertainty.

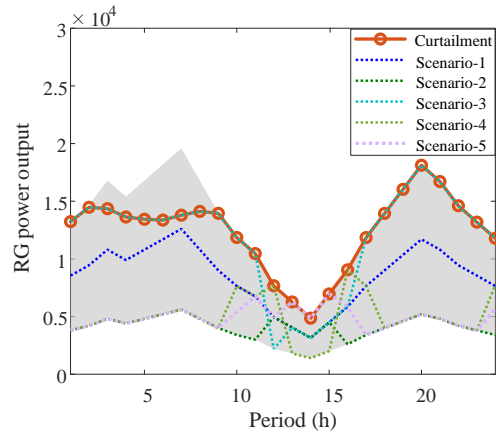


Fig. 10. Optimal pre-dispatch curtailment and worst-case scenarios of the Guangdong system.

2) The proposed algorithm can reduce the computational time by 95% compared with the nested C&CG algorithm.

3) With higher uncertainty, the performance of the proposed algorithm remains stable while the number of iterations needed by the nested C&CG is less predictable.

4) Compared with the traditional model with real-time curtailment only, the proposed model can avoid significant wind curtailments in the re-dispatch stage and can also lower the amount of reserve required.

APPENDIX

A. Redundancy Elimination

A redundant constraint in $\mathcal{W}(\xi)$ is defined as follows.

Definition A1. (Redundant Constraint) Given ξ and z^* , a constraint is *redundant* if removing that constraint does not change the uncertainty set $\mathcal{W}(\xi)$.

Denote $Q := [H, -C]$, $u := [w^\top, \hat{w}^\top]^\top$, and $q := F\xi + Gz^* + a$. Then the redundant constraints can be removed with the help of the following theorem.

Theorem A1. Constraint $Q_j u \leq q_j$ is redundant if the following linear program has a feasible solution

$$v^\top Q_{[-j]} = Q_j, \quad q_j \geq v^\top q_{[-j]}, \quad v \geq 0 \quad (\text{A.1})$$

Proof. If constraint $Q_j u \leq q_j$ is redundant, the polytope $\{u | Q_{[-j]} u \leq q_{[-j]}\}$ defined by the remaining constraints must be a subset of $\{u | Q_j u \leq q_j\}$. Therefore, we have $\{u | Q_{[-j]} u \leq q_{[-j]}\} \cap \{u | Q_j u > q_j\} = \emptyset$. According to the Nonhomogeneous Farkas Lemma [35], it is equivalent to

$$Q = \{v | v^\top Q_{[-j]} = Q_j, \quad q_j \geq v^\top q_{[-j]}, \quad v \geq 0\} \neq \emptyset \quad (\text{A.2})$$

In other words, the corresponding linear program has a feasible solution. \square

By checking each of the constraints in $\mathcal{W}(\xi)$, remove the redundant ones, and identify the active constraints, we can avoid the primal degeneracy.

B. Proof of Theorem 1

We start the proof of Theorem 1 with the following lemma.

Lemma B1. Suppose the optimal solution of (6) is (x^*, ξ^*) . Let N be the iteration run of Algorithm 1. For any $n \in [N]$:

- (a) $LB_n \leq c^\top x^* + g(\xi^*) + S(x^*, \xi^*) \leq UB_n$
- (b) For any $n_1, n_2 \in [N-1]$, the set of active constraints \mathcal{AC}_{n_1} won't be the same as the set of active constraints \mathcal{AC}_{n_2} .
- (c) If there exists some $n \in [N-1]$ whose set of active constraints \mathcal{AC}_n is the same as \mathcal{AC}_N , the algorithm terminates in N .

Proof. Assertion (a): For each $n \in [N]$, constraints (15d) and (15e) give a feasible point of $\mathcal{W}(\xi)$. The robust optimization problem (6) can be equivalently written as

$$\min_{x, \xi} c^\top x + g(\xi) + \eta \quad (\text{B.1a})$$

$$\text{s.t. } x \in \mathbb{X}, \xi \in \Xi \quad (\text{B.1b})$$

$$\eta \geq Q(x, w), \forall w \in \mathcal{W}(\xi) \quad (\text{B.1c})$$

while the master problem **MP** is

$$\min_{x, \xi} c^\top x + g(\xi) + \eta \quad (\text{B.2a})$$

$$\text{s.t. } x \in \mathbb{X}, \xi \in \Xi \quad (\text{B.2b})$$

$$\eta \geq Q(x, w), \forall w \in \Gamma(\text{Sol}(\mathcal{AC}_n, \xi)) \quad (\text{B.2c})$$

where $\text{Sol}(\mathcal{AC}_n, \xi)$ refers to the unique solution of the set of active constraints \mathcal{AC}_n given ξ and $\Gamma(\cdot)$ refers to the projection exerted by (15e). Then, w^n is a feasible point of $\mathcal{W}(\xi)$. The two problems (B.1) and (B.2) have the same objective functions while the constraint (B.2c) is a relaxation of (B.1c). Therefore, the optimal value of (B.2), i.e., LB_n , is no more than that of (B.1), i.e., $c^\top x^* + g(\xi^*) + S(x^*, \xi^*)$. Next, we prove $UB_n \geq c^\top x^* + g(\xi^*) + S(x^*, \xi^*)$ by induction. First of all, $UB_0 > c^\top x^* + g(\xi^*) + S(x^*, \xi^*)$. Suppose for the sake of induction that $UB_{n-1} > c^\top x^* + g(\xi^*) + S(x^*, \xi^*)$. Then if $S_f(x^{n*}, \xi^{n*}) > 0$, we have $UB_n = UB_{n-1} > c^\top x^* + g(\xi^*) + S(x^*, \xi^*)$; else, (x^{n*}, ξ^{n*}) is robust feasible and we have $UB_n = c^\top x^{n*} + g(\xi^{n*}) + S(x^{n*}, \xi^{n*})$. Due to the optimality of (x^*, ξ^*) , we have $UB_n \geq c^\top x^* + g(\xi^*) + S(x^*, \xi^*)$.

Assertion (b): If we have \mathcal{AC}_{n_1} be the same as \mathcal{AC}_{n_2} , then, $w^{n_2*} = \Gamma(\text{Sol}(\mathcal{AC}_{n_2}, \xi^{n_2*})) = \Gamma(\text{Sol}(\mathcal{AC}_{n_1}, \xi^{n_2*}))$. This also implies that (x^{n_2*}, ξ^{n_2*}) is robust feasible, so we have $UB_{n_2} = c^\top x^{n_2*} + g(\xi^{n_2*}) + Q(x^{n_2*}, w^{n_2*})$. Moreover, η in the master problem is the maximum of $Q(x^{n_2*}, w)$ for all $w = \Gamma(\text{Sol}(\mathcal{AC}_j, \xi^{n_2*}))$, $j = [n_2 - 1]$. so $\eta \geq Q(x^{n_2*}, w^{n_1*}) = Q(x^{n_2*}, w^{n_2*})$. Therefore, $LB_{n_2} \geq UB_{n_2}$. Together with $UB_{n_2} \geq LB_{n_2}$, we have $LB_{n_2} = UB_{n_2}$, and the algorithm terminates in the n_2 iteration, which is contradict to the fact that $N > n_2$ is the iteration run.

Assertion (c): Following a similar procedure as in the proof of (b), it is easy to get (c). \square

Now the proof of **Theorem 1** is given below.

First, we prove that the algorithm terminates in a finite number of iterations. According to Lemma B1(b)-(c), the same set of active constraints won't be attached twice. Moreover, each set of active constraints is composed of $4N_w \times T$ linearly-independent constraints from $\mathcal{W}(\xi)$. Since there are a finite

number of those possible combination of constraints, when A1 holds, the algorithm will terminate in finite steps.

Next, we show the robust feasibility of (x^{N*}, ξ^{N*}) . Since (x^{N*}, ξ^{N*}) is generated by the **MP**, we have $x^{N*} \in \mathbb{X}$ and $\xi^{N*} \in \Xi$. Also, the algorithm terminates when $S_f(x^{N*}, \xi^{N*}) = 0$, so for any $w \in \mathcal{W}(\xi^{N*})$, the second-stage problem (5) is feasible.

Finally, we show the optimality of (x^{N*}, ξ^{N*}) . According to Lemma B1(a), we have $LB_N \leq c^\top x^* + g(\xi^*) + S(x^*, \xi^*) \leq UB_N$. Together with the condition for termination $|UB_N - LB_N| \leq \varepsilon$. Therefore,

$$\begin{aligned} & |c^\top x^N + g(\xi^N) + S(x^N, \xi^N) - (c^\top x^* + g(\xi^*) + S(x^*, \xi^*))| \\ &= |UB_N - (c^\top x^* + g(\xi^*) + S(x^*, \xi^*))| \\ &\leq |UB_N - LB_N| \leq \varepsilon \end{aligned} \quad (\text{B.3})$$

which justifies the optimality of (x^{N*}, ξ^{N*}) . \square

REFERENCES

- [1] Global Wind Energy Council, "GWEC-global wind report 2021," 2021, [Online]. Available: <https://gwec.net/wp-content/uploads/2021/03/GWEC-Global-Wind-Report-2021.pdf>.
- [2] Global Solar Council, "Global market outlook for solar power 2021–2025," 2021, [Online]. Available: https://www.infobuildenergia.it/wp-content/uploads/2020/06/SolarPower-Europe_Global-Market-Outlook-for-Solar-2021-2025_V3.pdf.
- [3] W. Wei, F. Liu, S. Mei, and Y. Hou, "Robust energy and reserve dispatch under variable renewable generation," *IEEE Trans. Smart Grid*, vol. 6, no. 1, pp. 369–380, Jan. 2015.
- [4] Y. Fu, M. Liu, and L. Li, "Multiobjective stochastic economic dispatch with variable wind generation using scenario-based decomposition and asynchronous block iteration," *IEEE Trans. Sustain. Energy*, vol. 7, no. 1, pp. 139–149, Jan. 2016.
- [5] Z. Hu, Y. Xu, M. Korkali, X. Chen, L. Mili, and J. Valinejad, "A Bayesian approach for estimating uncertainty in stochastic economic dispatch considering wind power penetration," *IEEE Trans. Sustain. Energy*, vol. 12, no. 1, pp. 671–681, Jan. 2021.
- [6] A. Lorca and X. A. Sun, "Adaptive robust optimization with dynamic uncertainty sets for multi-period economic dispatch under significant wind," *IEEE Trans. Power Syst.*, vol. 30, no. 4, pp. 1702–1713, Jul. 2015.
- [7] Y. Chen, W. Wei, F. Liu, and S. Mei, "Distributionally robust hydro-thermal-wind economic dispatch," *Appl. Energy*, vol. 173, pp. 511–519, Jul. 2016.
- [8] W. Wei, F. Liu, and S. Mei, "Distributionally robust co-optimization of energy and reserve dispatch," *IEEE Trans. Sustain. Energy*, vol. 7, no. 1, pp. 289–300, Jan. 2016.
- [9] D. Bertsimas, E. Litvinov, X. A. Sun, J. Zhao, and T. Zheng, "Adaptive robust optimization for the security constrained unit commitment problem," *IEEE Trans. Power Syst.*, vol. 28, no. 1, pp. 52–63, Feb. 2013.
- [10] B. Zeng and L. Zhao, "Solving two-stage robust optimization problems using a column-and-constraint generation method," *Oper. Res. Letters*, vol. 41, no. 5, pp. 457–461, Sep. 2013.
- [11] S. Liu, Z. Bie, J. Lin, and X. Wang, "Curtailement of renewable energy in northwest China and market-based solutions," *Energy Policy*, vol. 123, pp. 494–502, Dec. 2018.
- [12] Z. Wu, P. Zeng, X.-P. Zhang, and Q. Zhou, "A solution to the chance-constrained two-stage stochastic program for unit commitment with wind energy integration," *IEEE Trans. Power Syst.*, vol. 31, no. 6, pp. 4185–4196, Nov. 2016.
- [13] G. Morales-España, Á. Lorca, and M. M. de Weerd, "Robust unit commitment with dispatchable wind power," *Electr. Power Syst. Res.*, vol. 155, pp. 58–66, Feb. 2018.
- [14] Y. Yang, W. Wu, B. Wang, and M. Li, "Chance-constrained economic dispatch considering curtailment strategy of renewable energy," *IEEE Trans. Power Syst.*, vol. 36, no. 6, pp. 5792–5802, Nov. 2021.
- [15] A. G. Abo-Khalil, "Impacts of wind farms on power system stability," in *Modeling and Control Aspects of Wind Power Systems*. IntechOpen, 2013.
- [16] J. Rogers, S. Fink, and K. Porter, "Examples of wind energy curtailment practices," National Renewable Energy Lab.(NREL), Golden, CO (United States), Tech. Rep., 2010, [Online]. Available: <https://www.nrel.gov/docs/fy10osti/48737.pdf>.

- [17] W. Yin, Y. Xue, S. Lei, and Y. Hou, "Multi-stage stochastic planning of wind generation considering decision-dependent uncertainty in wind power curve," in *2019 IEEE PES Innov. Smart Grid Technol. Conf. Eur. (ISGT-Eur.)*. IEEE, Oct. 2019, pp. 1–5.
- [18] B. Tarhan, I. E. Grossmann, and V. Goel, "Stochastic programming approach for the planning of offshore oil or gas field infrastructure under decision-dependent uncertainty," *Ind. Eng. Chem. Res.*, vol. 48, no. 6, pp. 3078–3097, Feb. 2009.
- [19] Y. Zhan, Q. P. Zheng, J. Wang, and P. Pinson, "Generation expansion planning with large amounts of wind power via decision-dependent stochastic programming," *IEEE Trans. Power Syst.*, vol. 32, no. 4, pp. 3015–3026, Jul. 2017.
- [20] O. Nohadani and K. Sharma, "Optimization under decision-dependent uncertainty," *SIAM J. on Optim.*, vol. 28, no. 2, pp. 1773–1795, 2018.
- [21] N. H. Lappas and C. E. Gounaris, "Robust optimization for decision-making under endogenous uncertainty," *Comput. Chem. Eng.*, vol. 111, pp. 252–266, Mar. 2018.
- [22] P. Vayanos, A. Georghiou, and H. Yu, "Robust optimization with decision-dependent information discovery," 2020, [Online]. Available: arXiv:2004.08490.
- [23] S. Avraamidou and E. N. Pistikopoulos, "Adjustable robust optimization through multi-parametric programming," *Optim. Lett.*, vol. 14, no. 4, pp. 873–887, May 2020.
- [24] Y. Zhang, F. Liu, Z. Wang, Y. Su, W. Wang, and S. Feng, "Robust scheduling of virtual power plant under exogenous and endogenous uncertainties," *IEEE Trans. Power Syst.*, vol. 37, no. 2, pp. 1311–1325, Mar. 2021.
- [25] Y. Zhang, F. Liu, Y. Su, Y. Chen, Z. Wang, and J. P. Catalão, "Two-stage robust optimization under decision dependent uncertainty," *IEEE/CAA J. Autom. Sin.*, 2022.
- [26] Y. Su, Y. Zhang, F. Liu, S. Feng, Y. Hou, and W. Wang, "Robust dispatch with demand response under decision-dependent uncertainty," in *2020 IEEE Sustain. Power Energy Conf. (iSPEC)*. IEEE, Nov. 2020, pp. 2122–2127.
- [27] L. Hellemo, P. I. Barton, and A. Tomasgard, "Decision-dependent probabilities in stochastic programs with recourse," *Comput. Manag. Sci.*, vol. 15, no. 3, pp. 369–395, Aug. 2018.
- [28] B. Zeng and W. Wang, "Two-stage robust optimization with decision dependent uncertainty," 2022, [Online]. Available: arXiv:2203.16484.
- [29] Z. Li, W. Wu, B. Zhang, and B. Wang, "Adjustable robust real-time power dispatch with large-scale wind power integration," *IEEE Trans. Sustain. Energy*, vol. 6, no. 2, pp. 357–368, Apr. 2015.
- [30] L. Wu, "A tighter piecewise linear approximation of quadratic cost curves for unit commitment problems," *IEEE Trans. Power Syst.*, vol. 26, no. 4, pp. 2581–2583, Nov. 2011.
- [31] J. Fortuny-Amat and B. McCarl, "A representation and economic interpretation of a two-level programming problem," *J. Oper. Res. Soc.*, vol. 32, no. 9, pp. 783–792, Sep. 1981.
- [32] R. T. Rockafellar, *Convex analysis*. Princeton university press, 2015.
- [33] L. Zhao and B. Zeng, "An exact algorithm for two-stage robust optimization with mixed integer recourse problems," *Tech. Rep.*, Jan. 2012, [Online]. Available: http://www.optimization-online.org/DB_FILE/2012/01/3310.pdf.
- [34] *Data Sheet*, Accessed: Mar. 28, 2022. [Online]. Available: <https://sites.google.com/site/yuechenth/data-sheet>.
- [35] Z. Xu, "Generalization of nonhomogeneous Farkas' Lemma and applications," *J. Math. Anal. Appl.*, vol. 186, no. 3, pp. 726–734, Sep. 1994.